COLORADO
Department of Transportation

CDOT Office of Applied Research

Development of Autonomous Truck Mounted Attenuator (ATMA) Deployment Guidelines Considering Traffic and Safety Impacts

Xianbiao Hu, Qing Tang, Yuxin Ding, Zirui Wu, Heather Pickering-Hilgers

August 2025

CDOT-2025-07

Technical Report Documentation Page

1. Report No.	2. Government Accession No.	3. Recipient's Catalog No.
CDOT-2025-07		

4. Title and Subtitle	5. Report Date
Development of Autonomous Truck Mounted Attenuator (ATMA) Deployment Guidelines Considering Traffic and Safety Impacts	June 2025
	6. Performing Organization Code

7. Author(s)	8. Performing Organization Report No.
Xianbiao Hu, Qing Tang, Yuxin Ding, Zirui Wu, Heather Pickering-Hilgers	

9. Performing Organization Name and Address	10. Work Unit No. (TRAIS)
Pennsylvania State University 282 ECoRE Building 556 White Course Dr, University Park, PA 16802	11. Contract or Grant No. SPR-5380-20-06

12. Sponsoring Agency Name and Address	13. Type of Report and Period Covered
Colorado Department of Transportation Office of Applied Research 2829 W. Howard Place Denver, CO 80204	14. Sponsoring Agency Code

15. Supplementary Notes

Prepared in cooperation with the pooled fund members of TPF 5(380) - Autonomous Maintenance Technology (AMT)

16. Abstract

The Autonomous Truck Mounted Attenuator (ATMA) system represents a specialized application of connected and autonomous vehicle (CAV) technologies, designed to enhance worker safety during roadway maintenance operations. Despite its growing adoption across state agencies, formalized deployment criteria remain absent from national guidelines such as the MUTCD, prompting individual DOTs to define their own standards. This study addresses a critical deployment challenge: identifying the appropriate traffic conditions—i.e., the Operational Design Domain (ODD)—under which ATMA can be safely and effectively used. The research begins by analytically modeling the reduced discharge rate resulting from ATMA-induced moving bottlenecks on multilane highways. Using this as a foundation, microscopic traffic simulation is applied to assess the resulting impacts on vehicle delay and traffic density—key metrics for determining Level of Service (LOS) as per the Highway Capacity Manual (HCM). Through this modeling framework, a functional relationship is established between Average Annual Daily Traffic (AADT) and LOS. The approach is validated using high-resolution NGSIM trajectory data, which confirms the model's ability to accurately reflect capacity reductions caused by slow-moving ATMA vehicles. Sensitivity analyses further reveal that roadway performance is highly influenced by K and D factors, as well as ATMA travel speed. Results suggest that, to maintain LOS at grade C, an AADT threshold of approximately 40,000 vehicles per day provides a practical design guideline.

17. Keywords	18. Distribution Statement
Autonomous Truck Mounted Attenuator (ATMA), Operational Design Domain (ODD), Automated Vehicle; Effective Discharge Rate; Moving Bottleneck	This document is available on CDOT's website: https://www.codot.gov/programs/research

19. Security Classif. (of this report)	20. Security Classif. (of this page)	21. No. of Pages	22. Price
Unclassified	Unclassified	38	

Acknowledgments

The contents of this report reflect the views of the authors, who are responsible for the facts and the accuracy of the information presented herein. This document is disseminated in the interest of information exchange. This report is funded, in whole or in part, by a grant from the Autonomous Maintenance Technology Pooled Fund administered by the Colorado Department of Transportation, along with matching funds provided by the U.S. Department of Transportation through the Mid-America Transportation Center. This report presents the research outcomes from the modeling and data analysis. However, neither the agencies nor the researchers assume any liability for its contents or their use

Table of Contents

List of Tables

List of Figures

List of Abbreviations and Acronyms

AMT..... Autonomous Maintenance Technology

ATMA.... Autonomous Truck Mounted Attenuator

ADS..... Automated Driving System

CAV..... Connected and Autonomous Vehicle

CTE..... Cross Track Error

DOT..... Department of Transportation

FT..... Follower Truck

GPS..... Global Positioning System

LT..... Lead Truck

MoDOT.. Missouri Department of Transportation

OCU..... Operator Control Unit

RF..... Radio Frequency

SAF..... Sensitivity Analysis Factor

SCU..... System Control Unit

UI..... User Interface

V2V..... Vehicle-to-Vehicle

Executive Summary

The Autonomous Truck Mounted Attenuator (ATMA) system represents a specialized application of connected and autonomous vehicle (CAV) technologies, designed to enhance worker safety during roadway maintenance operations. Despite its growing adoption across state agencies, formalized deployment criteria remain absent from national guidelines such as the MUTCD, prompting individual DOTs to define their own standards. This study addresses a critical deployment challenge: identifying the appropriate traffic conditions—i.e., the Operational Design Domain (ODD)—under which ATMA can be safely and effectively used. The research begins by analytically modeling the reduced discharge rate resulting from ATMA-induced moving bottlenecks on multilane highways. Using this as a foundation, microscopic traffic simulation is applied to assess the resulting impacts on vehicle delay and traffic density—key metrics for determining Level of Service (LOS) as per the Highway Capacity Manual (HCM). Through this modeling framework, a functional relationship is established between Average Annual Daily Traffic (AADT) and LOS. The approach is validated using high-resolution NGSIM trajectory data, which confirms the model's ability to accurately reflect capacity reductions caused by slow-moving ATMA vehicles. Sensitivity analyses further reveal that roadway performance is highly influenced by K and D factors, as well as ATMA travel speed. Results suggest that, to maintain LOS at grade C, an AADT threshold of approximately 40,000 vehicles per day provides a practical design guideline.

Chapter 1. Problem Statement and Significance

The U.S. highway network plays a vital role in facilitating the movement of people and goods across the country. However, continual usage and aging infrastructure have led to deteriorating road conditions, with approximately 43% of public roadways classified as being in poor or mediocre condition [1]. In 2020 alone, the U.S. Department of Transportation (USDOT) invested $24 billion in highway preservation efforts. Essential but low-speed maintenance tasks—such as striping, sweeping, pothole repair, and bridge cleaning—are necessary for maintaining operational safety and efficiency. Unfortunately, these operations often expose state Department of Transportation (DOT) crews to elevated crash risks. For instance, in Missouri, over 80 crashes involving slow-moving maintenance vehicles have been recorded since 2013, many resulting in injuries to DOT personnel [2]. Finding effective strategies to mitigate these hazards remains a pressing concern.

One promising technological response is the Autonomous Truck Mounted Attenuator (ATMA) system, which integrates connected and autonomous vehicle (CAV) technologies under the broader umbrella of Autonomous Maintenance Technology (AMT). ATMA is a specialized leader–follower system that eliminates the need for a human driver in the rear maintenance truck, thereby reducing the exposure of DOT workers to potential collisions in work zones. Initiatives by states such as Colorado and Missouri have led early adoption efforts, and several other states—including California, Virginia, Ohio, North Dakota, Minnesota, and Tennessee—are also piloting or deploying similar systems [3-5]. Additionally, Colorado DOT is spearheading a multi-state AMT pooled fund project in collaboration with 17 member DOTs and the FHWA [6]. A technical overview of ATMA's system configuration is provided in Section 2.

While the technology is rapidly gaining traction, established and uniform deployment guidance is absent from national standards such as the Manual on Uniform Traffic Control Devices (MUTCD). As a result, individual states are developing their own criteria to determine where and when ATMA can be implemented. For instance, Colorado DOT currently uses a threshold of 6,000 vehicles per day in Annual Average Daily Traffic (AADT) to identify suitable low-volume roads. This threshold is based on the concern that ATMA vehicles—operating at slow speeds of 5 to 15 mph—might impede traffic flow on high-demand corridors. However, this AADT value may not be suitable in all contexts, especially in states like California or New York where traffic volumes are generally much higher. This raises an important question: Is the 6,000 AADT threshold scientifically defensible across different traffic environments, or should a more systematic method be developed?

To address this gap, this research develops a microscopic traffic modeling framework to define the Operational Design Domain (ODD) for ATMA systems operating on multilane highways. Drawing upon the Highway Capacity Manual (HCM) [7], which outlines six performance indicators for assessing the level of service (LOS)—including speed, delay, throughput, density, environmental conditions, and demand-to-capacity ratio—we focus specifically on delay and density as key metrics. Quantifying these metrics under ATMA operation hinges on accurately estimating the drop in roadway capacity caused by the system's low-speed movement. Due to its slower speed relative to general traffic, the ATMA system behaves as a moving bottleneck, warranting precise modeling of this effect before LOS impacts can be evaluated.

Existing literature has explored how moving bottlenecks affect roadway discharge rates. Leclercq et al. [8, 9] expanded upon the Newell-Daganzo model to simulate capacity drops resulting from vehicle merging. Further studies incorporated heterogeneity in vehicle characteristics and wave interactions, providing numerical—but not closed-form—solutions [10]. Yuan et al. [11] analyzed how acceleration variability and reaction time influence queue discharge rates, while Laval and Daganzo [12] modeled capacity losses stemming from lane-changing behaviors. Additional efforts by Chen and Ahn [13] and others [14-18] addressed bottleneck phenomena at merges, diverges, and weaves. However, most of these models are complex, lack generalizability, and do not yield explicit analytical expressions—challenges that make them less suitable for real-world deployment guidance. These limitations are particularly relevant for ATMA systems, which involve at least two vehicles (a manned leader and one or more unmanned followers) separated by gaps of 100–1,000 ft—distinctly different from conventional bottlenecks.

This study begins by analytically deriving the effective discharge rate associated with the ATMA-induced moving bottleneck, using a transformed fundamental diagram in a moving coordinate system. The resulting discharge rate expressions are closed-form, mathematically simple, and incorporate key variables such as traffic demand, prevailing traffic speed, ATMA speed, jam density, and backward wave speed. Once the reduced capacity is quantified, it is incorporated into a microscopic traffic flow model to compute both vehicle delay and density under varying demand scenarios. These outputs are then used to determine the LOS and to establish a robust relationship between AADT and service level. Ultimately, the approach supports data-driven identification of ATMA's operational design domain.

This report is organized as follows:

- Section 2 provides background on the ATMA system, performance metrics for multilane highways, and an overview of discharge rate and queue formation modeling.
- Section 3 presents the methodology, including the analytical derivation of effective discharge rate and delay under moving bottleneck conditions.
- Section 4 offers validation of the proposed model using NGSIM data, followed by result analysis and sensitivity evaluations.
- Section 5 concludes the report.

Chapter 2. ATMA System Introduction and Fluid Queue Models

This section begins with an overview of the Autonomous Truck Mounted Attenuator (ATMA) system, followed by a review of level-of-service (LOS) performance metrics for multilane highways as defined in the Highway Capacity Manual (HCM). We then introduce the theoretical framework for modeling discharge rate using a triangular fundamental diagram, and describe how traffic delay and queue length can be analytically derived under varying traffic conditions.

A summary of notations used throughout the report is provided below:

Table 1. Summary of notations

Notation	Explanation
$\mathbf{t}$	timestamp
$\mathbf{n}, \mathbf{n-1}$	indexes of following and leading vehicle, respectively
$\boldsymbol{\tau_n}, \mathbf{d_n}$	response time and temporal delay of vehicle $\mathbf{n}$
$\mathbf{v_1}, \mathbf{v_2}$	speeds before and after the speed changes
$\mathbf{h_{n,1}}, \mathbf{h_{n,2}}$	time headway of vehicle $\mathbf{n}$ before and after the speed changes
$\mathbf{s_{n,1}}, \mathbf{s_{n,2}}$	space headway of vehicle $\mathbf{n}$ before and after the speed changes
$\mathbf{q}, \mathbf{k}, \mathbf{v}$	traffic flow, density and speed
$\bar{\boldsymbol{\tau}}, \bar{\mathbf{d}}$	arithmetic average of the $\boldsymbol{\tau}$ and $\mathbf{d}$
$\mathbf{v_f}, \mathbf{k_j}$	free-flow speed and jam density
$\mathbf{v_u}$	cruising speed on the four-lane highway segment. Due to bottleneck or congestion, $\mathbf{v_u} \leq \mathbf{v_f}$
$\mathbf{w}$	backward wave speed
$\boldsymbol{\mu}$	maximum discharge rate
$\boldsymbol{\lambda(t)}$	time-dependent arrival rate
$\mathbf{t_0}, \mathbf{t_1}$	time that queue starts, and time to reach the maximum arrival rate
$\mathbf{t_2}, \bar{\mathbf{t}}$	time with longest queue, and time when the queue is fully discharged
$\mathbf{Q(t)}$	time-dependent queue length

Notation	Explanation
W	total delay
N	total number of vehicles that enter a roadway segment
v_{lt}	speed of the ATMA vehicles
θ	discount factor of the effective discharge rate
$x^*(t)$	location of a moving observer relative to the entering vehicle
$q^*(t)$	flow rate at which vehicle pass the observer who is travelling at a speed of $v^*(t)$
$Q(k)$, $Q^*(k)$	flow as a function of density seen from stationary and moving coordinates
$\lambda_{in}(t), \lambda'_{in}(t)$	adjusted flow rate from stationary coordinate and moving coordinate
APE	absolute percentage error
$\bar{W}$	average delay during the AMTA vehicles performing maintenance
$\bar{t}$	average travel time on the four-lane highway segment
$\tilde{k}$	estimated density on the four-lane highway

2.1. ATMA Vehicle System Overview

The Autonomous Truck Mounted Attenuator (ATMA), also known as the Autonomous Impact Protection Vehicle (AIPV), is a new-generation technology aimed at improving safety during highway maintenance. As illustrated in Figure 1, the ATMA configuration typically includes a human-driven lead truck and an autonomous follower truck equipped with a Truck Mounted Attenuator (TMA). The follower vehicle trails the lead truck at a short distance (typically 100–200 feet), mimicking its trajectory while providing a protective buffer in the event of rear-end collisions.

This leader–follower setup simplifies the autonomous control requirements by allowing the follower to replicate the leader's movements, thereby reducing system complexity. In the event of an unavoidable crash in a work zone, the follower truck—devoid of human occupants and equipped with the TMA—absorbs the impact, effectively shielding DOT workers. V2V communications, onboard control units, software, and sensors integrated into both vehicles enable this coordinated operation.

(a)

(b)

(c)

Figure 1. ATMA Vehicle System: (a) system overview; (b) view from above; and (c) view from the rear.

2.2. Performance Measurement of Multilane Highways

Level of Service (LOS) is a structured framework for quantifying traffic performance and user experience. As outlined in HCM [7], six key indicators are used to assess LOS on multilane roadways:

- Density: Vehicles per lane per mile;
- Speed: Average travel speed;
- Volume-to-Capacity Ratio (v/c): Measure of congestion level;
- Delay: Deviation from free-flow conditions;
- Throughput: Volume processed by the system;
- Environmental Impacts: e.g., emissions.

Figure 2 illustrates how LOS categories are linked to traffic speed and density, given a particular free-flow speed (FFS). This relationship holds under typical conditions. However, when ATMA vehicles are present, they induce moving bottlenecks that reduce effective capacity and disrupt the usual flow-speed relationship. To assess the impact of these disruptions, a more detailed model accounting for capacity

reductions is necessary. Once adjusted capacity is determined, microscopic traffic models can estimate both delay and density, allowing LOS to be evaluated against standard HCM thresholds.

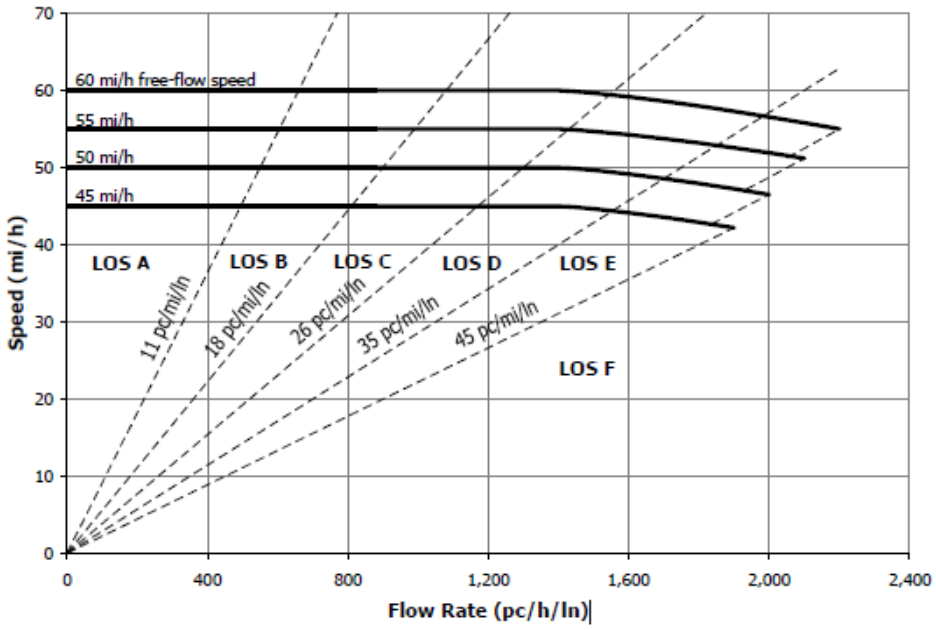

Figure 2. LOS on Base Speed-Flow curves from HCM (2010).

2.3. Discharge Rate Under Normal Traffic Conditions

This section presents how traffic discharge rate—or effective capacity—is calculated under typical conditions. We adopt a simplified car-following model originally proposed by Newell [19], which assumes that a following vehicle mirrors the trajectory of its leader with a fixed temporal and spatial lag. As shown in Figure 3-a below, the time-space trajectory of a following vehicle n is essentially the same as its leading vehicle $n-1$, except for a delay in space and in time. In the time-space diagram (shown in Figure 3-a below), a leading vehicle $n-1$ initially drives at a constant speed v_1 and then changes to another constant speed v_2. According to the simplified car-following model, the following vehicle n also travels at the same speed of v_1 at the beginning, and then changes to the v_2 speed. However, at the turning point, there is a temporal delay of τ_n which represents the driver n's necessary response time, as well as a spatial delay of d_n, which represents the distance needed to ensure safe driving.

Following vehicle n's movement trajectory can be calculated by $x_n(t+\tau_n) = x_{n-1}(t) + d_n$. Based on the time-space diagram, the time headway of n's vehicle, before and after speed change, can be derived with $h_{n,1} = \tau_n + \frac{d_n}{v_1}$ and $h_{n,2} = \tau_n + \frac{d_n}{v_2}$, respectively. The space headway of n's vehicle, before and after the speed changes, can be computed by $s_{n,1} = d_n + \tau_n \cdot v_1$ and $s_{n,2} = d_n + \tau_n \cdot v_2$, respectively.

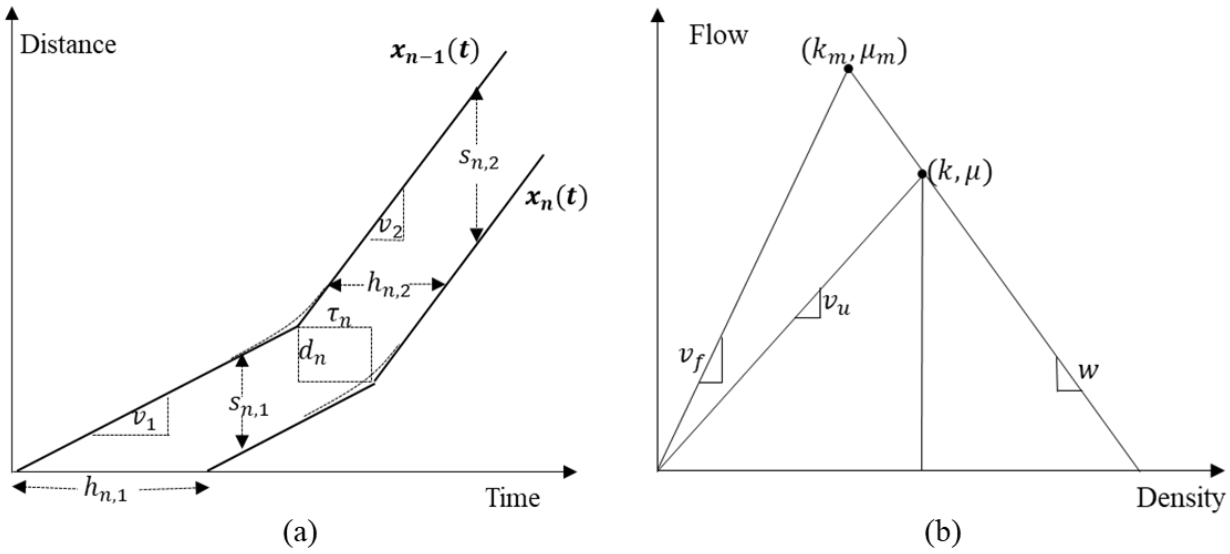

Figure 3. (a) Time-space diagram of Newell's car-following model and (b) triangular fundamental diagram.

The Newell car-following model above suggests the triangular fundamental diagram that is shown in Figure 3-b. Per [19], the q-k relationship can be represented as $q = \frac{1}{\bar{\tau}} - \frac{\bar{d}}{\bar{\tau}}k$, in which $\bar{\tau} = \frac{1}{n}\sum_{k=1}^{n} \tau_k$ and $\bar{d} = \frac{1}{n}\sum_{k=1}^{n} d_k$.The fundamental diagram has a free flow speed v_f, backward wave speed w, maximum discharge rate μ_m and its corresponding density k_m, and jam density k_j. Of the five variables, if three of them are known, the remaining two can be derived.

Following the above-mentioned fundamental diagram, when v_f, w, and k_j are known for a roadway segment, its maximum discharge rate μ_m can be calculated as $\mu_m = \frac{k_j}{(\frac{1}{v_f}+\frac{1}{w})} = \frac{k_j \cdot v_f \cdot w}{v_f + w}$. It should be noted that μ_m is the maximum discharge rate under prevailing traffic conditions. In the case of congestion (e.g., due to lane drop or other geometric reasons), the actual cruising speed may be lower than the free-flow speed. We used a new point (k, μ) in the q-k diagram in Figure 3-b to represent the discharge rate due to the congestion impact, with $\mu < \mu_m$. The cruising speed is denoted as v_u, with $v_u < v_f$, the new discharge rate becomes Equation 1 in a generic form.

$$\mu = \frac{k_j}{(\frac{1}{v_u}+\frac{1}{w})} = \frac{k_j \cdot v_u \cdot w}{v_u + w}$$

Equation 1. Derivation of Discharge Rate

2.4. Queue Length and Delay

Newell's fluid-based approximation [20] is used here to characterize traffic queues during peak demand. The system is treated as being in either a free-flow or congested state. When the time-varying demand λ(t) exceeds capacity μ, queues form and delay accumulates.

We denote the time-dependent arrival rate (i.e., the demand) as $\lambda(t)$. During off-peak hours, $\lambda(t) < \mu$ and no queue exists (to be exact, when a moving bottleneck is present, the discounted capacity μ' should be used, but for the sake of simplicity, we still use μ here). When the demand increases and finally exceeds the μ, vehicles start to form a queue. The queue dissipates and traffic returns to normal, as demand reduces after peak hours. Figure 4 provides an illustration of the demand-supply relationship and queuing profile. In Figure 4(a), the demand (black curve OABCE) exceeds the maximum discharge rate (red horizontal line AD) during the peak hour between t_0 and t_2, and the queue formation is illustrated by the area highlighted by red lines (i.e., ABCA). The arrival rate reaches peak at time t_1. The longest queue is observed at time t_2 and starts to shrink, as shown by the green lines (i.e., area CDEC). The queue is fully discharged at time $\bar{t}$. The queuing profile is illustrated in Figure 4(b).

Based on the illustration in Figure 4, the length of the queue at time t can be derived by $Q(t) = \int_{t_0}^{t}(\lambda(\tau) - \mu)d\tau$. The total delay is, thus, the integral of queue length from t_0 to t_3, which can be calculated by Equation 2.

$$W = \int_{t_0}^{t_3} Q(t)d\tau = \int_{t_0}^{\bar{t}} Q(t)d\tau$$

Equation 2. Derivation of Total Delay

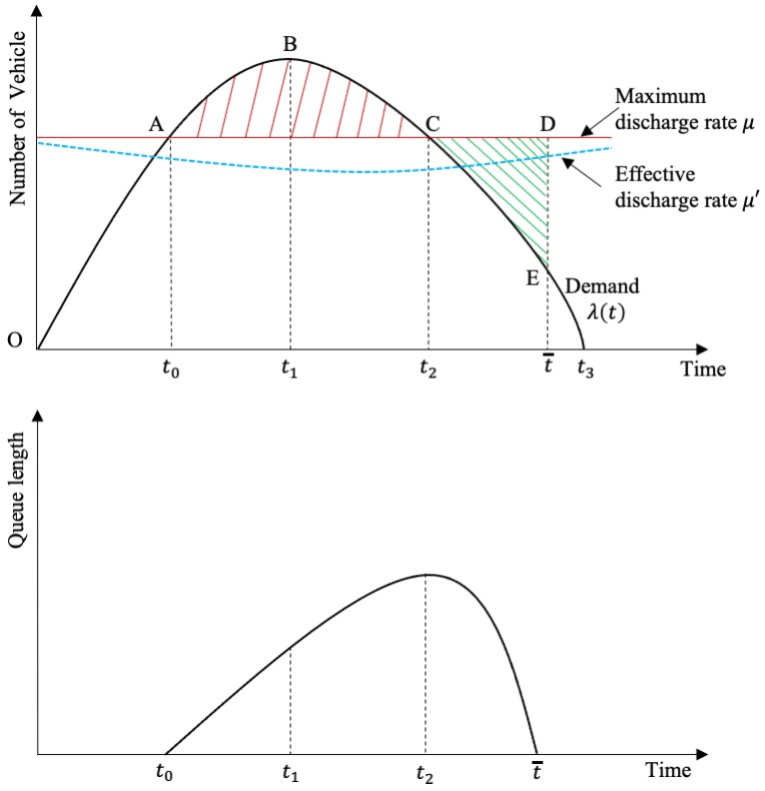

Figure 4. Queue formation and dissipation processes.

Chapter 3. Modeling Methodologies

3.1. Problem Definition

This section presents a representative highway scenario consisting of two lanes traveling in the same direction. As illustrated in Figure 5, an ATMA system is modeled as a leader-follower vehicle pair, with a manned lead truck (LT) and an unmanned follower truck (FT), separated by a fixed gap L_{gap}. General traffic is depicted as smaller black vehicle icons.

The total in-flow rate is $\lambda(t)$ for both lanes. The lane flow distribution is presented by α, so the left lane has a flow rate of $\alpha * \lambda(t)$, whereas the right-lane has a flow rate of $(1-\alpha) * \lambda(t)$. The cruising speed of general traffic is v_u, and ATMA vehicles drive at a constant speed of v_{lt} (with lt standing for leader truck). v_{lt} is usually between 5~15mph and is, thus, much slower than v_u, i.e., $v_{lt} < v_u$ and, as such, the ATMA can be considered as a moving bottleneck in the two-lane highway segment. As a result, the vehicles behind the ATMA vehicles (represented by red colored small cars in Figure 5) can switch to the left lane to bypass the moving bottleneck. Note that, although for simplicity a two-lane highway is used, the proposed model can be iteratively applied to a highway with three or even more lanes.

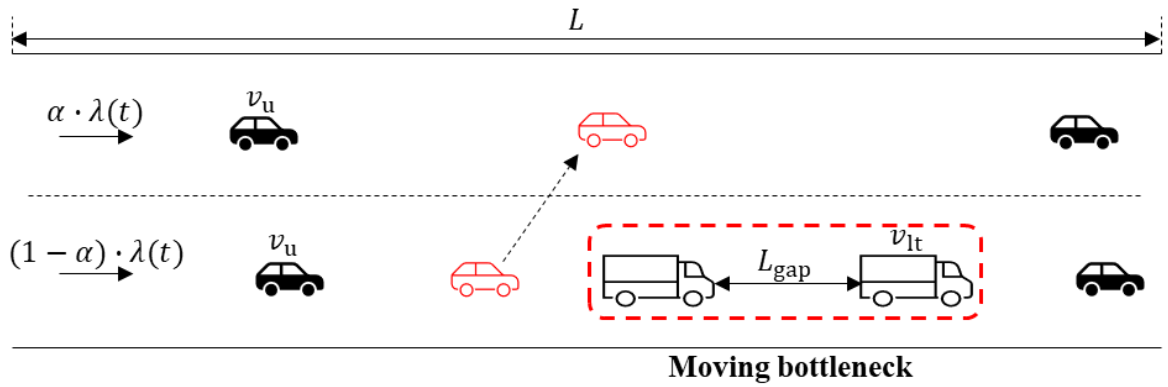

Figure 5. Schematic of a four-lane highway segment with an ATMA system acting as a moving bottleneck

3.2. Analytical Derivation of Capacity Reduction Due to Moving Bottleneck

To estimate the effective capacity during ATMA operation, we apply Newell's moving coordinate system approach [21]. By shifting the observer's frame of reference to travel at the same speed as the ATMA (v_{lt}), we convert the dynamic bottleneck problem into an equivalent stationary bottleneck scenario.

We start by placing a "moving observer" on the main road who is traveling at the same velocity v_{lt} as the ATMA vehicles, at any time t, at a location $x^*(t)$ relative to the ATMA vehicles. The equation from

Newell [21], on the derivation of $x^*(t)$, is given in Equation 3. In our problem, since they travel at the same speed, $x^*(t)$ remains a constant. Next, we also place a "stationary observer" on the main road, whose location does not change.

$$x^*(t) = x(t) - v_{lt} \cdot t$$

Equation 3. Location Change of the Moving Observer

As the moving observer moves at the same speed as the ATMA vehicles, from his perspective, the two-lane roadway segment becomes a stationary section of road with only one lane for the other vehicles adjacent to ATMA vehicles. From his perspective, there is a lane reduction with a capacity drop. Some vehicles merge from two lanes to one lane, pass this bottleneck location, and then switch lanes to drive again on a two-lane roadway segment (again, please refer to the red vehicles in Figure 5). Let us call the view from the moving observer's perspective "moving coordinates", and that from the stationary observer's perspective "stationary coordinates". Based on such definitions, the target of this section, i.e., the moving bottleneck capacity, is the maximum discharge rate from a stationary observer's perspective, with the presence of ATMA vehicles. Below we show how to derive such a value step by step.

Assume that the flow and the density of the one lane and two lanes have a functional relationship in the stationary coordinates, i.e. $q = Q_1(k)$ and $q = Q_2(k)$, if we use $q^*(t)$ to denote the rate at which vehicles on the main road pass the moving observer, who is travelling at a speed of v_{lt}, then

$$q^*(t) = q - k \cdot v_{lt}$$

Equation 4. Flow Rate Passing the Moving Observer

The density of the one-lane and the two-lane roadway segments are the same, no matter whose perspective (moving observer or stationary observer) is adopted. The relationship between $q^*(t)$ and k can be derived as:

$$q^*(t) = Q_1(k) - k \cdot v_{lt} = Q_1{}^*(k), \qquad q^*(t) = Q_2(k) - k \cdot v_{lt} = Q_2{}^*(k)$$

Equation 5. Relationship Between flow Rate and Density

In which $Q_1{}^*(k)$ and $Q_2{}^*(k)$ represent the q-k relationship of a one-lane and a two-lane roadway segment, as seen from the moving observer's perspective.

Figure 6 presents q-k fundamental diagrams of a one-lane and a two-lane roadway from both a moving observer's and a stationary observer's perspectives. The moving observer's view is marked with red (i.e., OGI), and the stationary observer's view is marked with black (i.e., OG'I'). The moving bottleneck's speed is fixed at v_{lt}. We start by noting that the triangle O-F-L is the fundamental diagram of the one-lane segment, and triangle O-G-I is the fundamental diagram of the two-lane segment in the moving coordinate. As discussed by Newell [21], if we add a flow of $k \cdot v_{lt}$ to q^*, the resulting FD will be in the stationary coordinates. As such, the triangle O-F'-L' is the fundamental diagram of the one-lane segment and triangle O-G'-I' is the fundamental diagram of the two-lane segment in the stationary coordinates. We have the angle of $\angle G'OI' = \arctan v_u$, angle of $\angle I'OI = \arctan v_{lt}$, and the angle of $\angle G'I'O = \arctan w$.

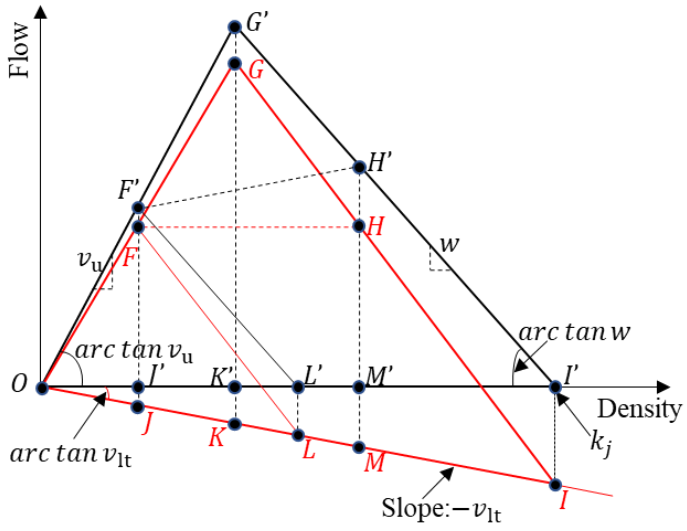

Figure 6. Flow-density relationship from both a moving observer's view and a stationary observer's view.

We first calculate the adjusted flow rate $\lambda_{in}{}'(t)$ in the moving coordinate system. At any given time t, we have an incoming flow rate $\lambda_{in}(t)$ and the moving bottleneck's speed v_{lt}. To convert that into the adjusted flow rate $\lambda_{in}{}'(t)$ in the moving coordinate system, we back calculate the density on the two-lane roadway segment with $Q_2(k_2) = \lambda_{in}(t)$, or $k_2 = Q_2{}^{-1}(\lambda_{in}(t))$. Then, the adjusted flow rate $\lambda_{in}{}'(t)$ can be calculated as

$$\lambda_{in}{}'(t) = \lambda_{in}(t) - k_2 \cdot v_{lt} = \lambda_{in}(t) - Q_2{}^{-1}(\lambda_{in}(t)) \cdot v_{lt}$$

Equation 6. Derivation of Adjusted Flow Rate

For example, in the stationary coordinate system, $F'J'$ is the maximum discharge rate of the one-lane segment, in which $F'J'$ is perpendicular to OI' and OJ' is its corresponding density. Following this, to calculate the maximum discharge rate of the one-lane segment in the moving coordinate system, we need to reduce $F'J'$ by $OJ' \cdot v_{lt}$ which is JJ' and, thus, becomes FJ'. In other words, FJ' is the maximum discharge rate of the one-lane segment in the moving coordinate system.

In the moving coordinate system, if $\lambda_{in}{}'(t) < FJ'$, all vehicles can pass through the moving bottleneck at full cruising speed v_u. Otherwise, the adjusted arrival rate $\lambda_{in}{}'(t)$ becomes higher than the maximum discharge rate and, thus, the ATMA vehicles become a moving bottleneck, and the roadway segment is subject to a maximum discharge rate with a value of FJ'. Subsequently, the traffic state of the downstream bottleneck location is represented by point F, while that of the bottleneck upstream is represented by point H, which has the same outflow rate as point F (i.e., $y_F = y_H$,) but with a higher density due to the queue. When we convert the moving coordinates back to the stationary coordinates points, F and H become points F' and H', after adding a flow of $k \cdot v_{lt}$, i.e. $y_{F'} = y_F + k_F v_{lt}$ and $y_{H'} = y_H + k_H v_{lt}$. Since the density at point H is higher than that at point F (i.e., $k_H > k_F$), the flow rate at point H' is also higher than that at point F' (i.e., $y_{H'} > y_{F'}$), Thus, it is point H' that determines the maximum discharge rate, instead of point F' in the stationary coordinate system.

Next, we derive the length of H'M', which is the maximum discharge rate of point H' in the stationary coordinate system (i.e., our target capacity with a moving bottleneck). First, let us look at the triangle of F-O-L, which is the fundamental diagram of a one-lane roadway. As $F'J'$ is the maximum discharge rate of the one-lane segment, we have $F'J' = \frac{\frac{k_j}{2}}{(\frac{1}{v_u}+\frac{1}{w})} = \frac{k_j \cdot v_u \cdot w}{2(v_u+w)}$. As the angle of $\angle G'OI' = \arctan v_u$, OJ' can be calculated as $OJ' = \frac{F'J'}{v_u} = \frac{k_j \cdot w}{2(v_u+w)}$. As the angle of $\angle G'I'O = \arctan w$, $J'L'$ can be calculated as $J'L' = \frac{F'J'}{w_m} = \frac{k_j \cdot v_u}{2(v_u+w)}$. As the angle of $\angle I'OI = \arctan v_{lt}$, JJ' can be calculated as $JJ' = OJ' \cdot v_{lt} = \frac{k_j \cdot w \cdot v_{lt}}{2(v_u+w)}$. Then, the maximum discharge rate of the moving bottleneck in the moving coordinates with a value of FJ' can be calculated as

$$FJ' = F'J' - JJ' = \frac{k_j \cdot v_u \cdot w}{2(v_u + w)} - \frac{k_j \cdot w \cdot v_{lt}}{2(v_u + w)} = \frac{k_j \cdot w \cdot (v_u - v_{lt})}{2(v_u + w)}$$

Equation 7. Derivation of Maximum Discharge Rate of the Moving Bottleneck

However, what we really need to calculate is the maximum discharge rate of point H' in the stationary coordinates, i.e., the length of $H'M'$. In the moving coordinates, we have the same flow at points F and H, which means that $HM' = FJ' = \frac{k_j \cdot w \cdot (v_u - v_{lt})}{2(v_u + w)}$. As $G'K'$ is the maximum discharge rate of the two-lane segment, we have $G'K' = \mu_m = \frac{k_j}{(\frac{1}{v_u} + \frac{1}{w})} = \frac{k_j \cdot v_u \cdot w}{v_u + w}$, and as the angle of $\angle G'I'O = \arctan w$, $K'I'$ can be calculated as $K'I' = \frac{G'K'}{w} = \frac{k_j \cdot v_u}{v_u + w}$.

Suppose the density at point H' is k, we have $w = \frac{H'M'}{M'I'} = \frac{HM' + kv_{lt}}{k_j - k} = \frac{\frac{k_j \cdot w \cdot (v_u - v_{lt})}{2(v_u + w)} + kv_{lt}}{k_j - k}$ and, thus, the density at point H' can be calculated as $k = \frac{k_j \cdot w}{2}(\frac{1}{v_u + w} + \frac{1}{v_{lt} + w})$. The effective discharge rate of point H' in the stationary coordinates, i.e., the length of $H'M'$can be calculated via Equation 8.

$$\mu' = H'M' = HM' + kv_{lt} = \frac{k_j \cdot w \cdot (v_u - v_{lt})}{2(v_u + w)} + \frac{k_j \cdot w \cdot v_{lt}}{2}\left(\frac{1}{v_u + w} + \frac{1}{v_{lt} + w}\right)$$
$$= \frac{k_j \cdot v_u \cdot w}{v_u + w} \cdot \frac{2v_{lt} \cdot v_u + w \cdot v_u + w \cdot v_{lt}}{2(v_{lt} + w) \cdot v_u} = \mu \cdot \frac{2v_u \cdot v_{lt} + v_{lt} \cdot w + w \cdot v_u}{2(v_{lt} + w) \cdot v_u}$$

Equation 8. Derivation of Effective Discharge Rate

In this way, the effective discharge rate of the moving bottleneck in the stationary system in Figure 6 has now been derived. If we use a new variable θ and make $\theta = \frac{2v_u \cdot v_{lt} + v_{lt} \cdot w + w \cdot v_u}{2(v_{lt} + w) \cdot v_u}$, Equation 8 becomes $\mu' = \mu \cdot \theta$, in which θ is, essentially, the capacity discount factor due to the moving bottleneck caused by the ATMA. In other words, before the ATMA vehicles enter the road, the roadway capacity is μ, and as soon as the ATMA vehicles enter the roadway segment, it creates a moving bottleneck with an effective discharge rate of μ', given by Equation 8, until the ATMA vehicles depart the roadway segment.

3.3. Derivation of Level of Service metrics

To assess ATMA's operational feasibility, we analyze two performance indicators: total delay and traffic density, in accordance with HCM guidance.

The main input data is the demand profile, i.e., AADT, and the K-factor (i.e., proportion of AADT occurring in the peak hour), as well as D-factor (i.e., the peak-hour volume proportion in the major

direction). HCM recommends that the peak 15-min flow rate is used for most of the analytical procedures, so the Peak Hour Factor (PHF) is also considered as an input.

To be consistent with the notations in the earlier sections, we use $\lambda(\tau)$ as the traffic demand input, considering the 15-min flow rate. Based on AADT, the K-factor, the D-factor, the hourly traffic demand $\lambda(\tau)$ can be derived by directional design hourly volume (DDHV) and PHF via Equation 9.

$$\lambda(\tau) = \frac{\mathrm{DDHV}}{\mathrm{PHF}} = \frac{\mathrm{AADT} \times \mathrm{K} \times \mathrm{D}}{\mathrm{PHF}}$$

Equation 9. Derivation of Hourly Traffic Demand

Next, by combining the discounted capacity from Equation 8 and demand profile from Equation 9, we derive the vehicle delay, as well as the traffic density, as follows.

First, the queue length during the ATMA maintenance can be calculated as $\mathrm{Q(t)} = \int_0^{\mathrm{t}} (\lambda(\tau) - \mu')\mathrm{d}\tau$, i.e., the number of vehicles sitting in the queue is the difference between demand and discharge rates.

Next, the total delay caused by the AMTA vehicles during maintenance on a roadway segment can be calculated as $\mathrm{W} = \int_0^{\frac{\mathrm{L}}{\mathrm{v_{lt}}}} \mathrm{Q(t)dt}$, in which L is the length of the roadway segment. The total number of vehicles that enter a roadway segment is $\mathrm{N} = \int_0^{\frac{\mathrm{L}}{\mathrm{v_{lt}}}} \lambda(\tau)\mathrm{d}\tau$. Thus, the average delay of each passenger vehicle can be computed as Equation 10.

$$\bar{\mathrm{W}} = \frac{\mathrm{W}}{\mathrm{N}} = \frac{\int_0^{\frac{\mathrm{L}}{\mathrm{v_{lt}}}} \mathrm{Q(t)dt}}{\int_0^{\frac{\mathrm{L}}{\mathrm{v_{lt}}}} \lambda(\tau)\mathrm{d}\tau}$$

Equation 10. Average Delay of Each Passenger Vehicle

Then, the average travel time on this four-lane highway segment can be calculated as Equation 11.

$$\bar{\mathrm{t}} = \frac{\mathrm{L}}{\mathrm{v_u}} + \bar{\mathrm{W}}$$

Equation 11. Average Travel Time on the Analyzed Four-Lane Highway

Now that the average travel time is known, we can easily convert it back to the average speed of a vehicle travelling on the roadway segment, and determine the density of the roadway segment. To do this, we first compute the average travel speed $\bar{v}$, as shown in Equation 12. Then, the density on this four-lane highway segment $\tilde{k}$ can be estimated as in Equation 13. Thus, the level of service on the

highway segment can be determined by looking up to HCM [7], or using the density thresholds in Figure 2.

$$\bar{v} = \frac{L}{\bar{t}}$$

Equation 12. Derivation of Average Travel Speed

$$\bar{k} = \frac{DDHV}{2\bar{v} \times PHF} = \frac{AADT \times K \times D}{2\bar{v} \times PHF}$$

Equation 13. Derivation of Density

Chapter 4. Case Studies

4.1. Validation of Effective Discharge Rate

To validate the effective discharge rate discount factor derived in Eq. (8), we utilize the NGSIM dataset, which provides high-resolution trajectory data for every vehicle on a roadway segment—ideal for assessing roadway capacity models. Our study focuses on northbound I-80 in Emeryville, California (Figure 7), particularly lanes 5 and 6 over a 1,090-foot stretch.

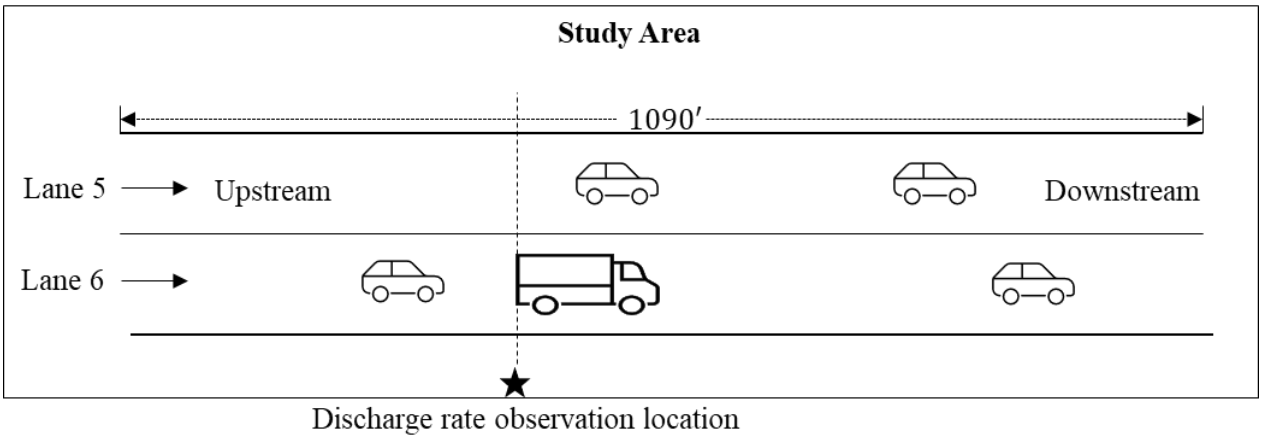

Figure 7. An illustration of the study area: Northbound I-80.

Using DTALite/NeXTA [22], an open-source tool, we extract critical parameters such as jam density, backward wave speed, and free-flow speed from the NGSIM dataset for two time periods on April 13, 2005: 4:00–4:15 PM and 5:00–5:30 PM. The time-space diagrams in Figure 8 reveal shockwave patterns highlighted by red boxes (A~E), with slopes indicating backward wave speeds averaging 12 mph. We set the jam density at 180 veh/lane/mile and free-flow speed at 30 mph. Applying Eq. (1), the maximum discharge rate is:

$$\mu = \frac{2k_j \cdot v_u \cdot w}{v_u + w} = 3{,}076\ veh/hr$$

Equation 14. Derivation of Maximum Discharge Rate from the Field

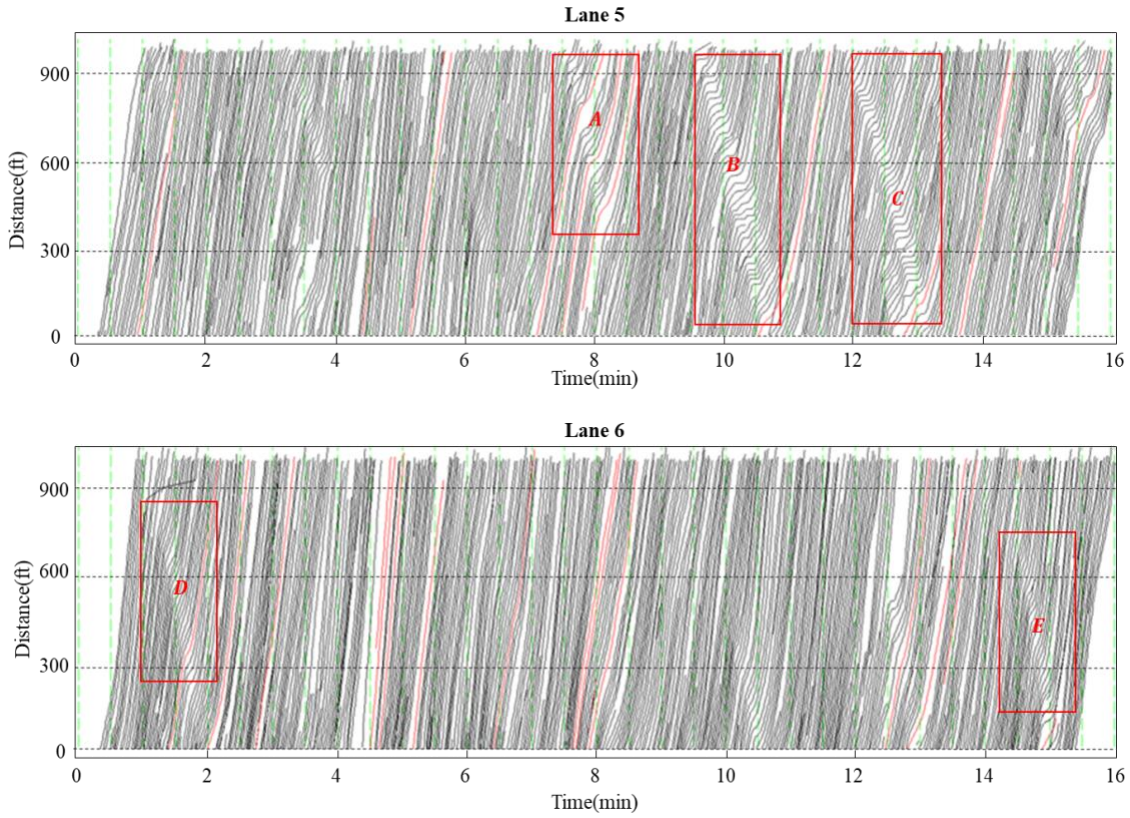

Figure 8. Vehicle trajectory for lanes 5 and 6, I-80, NGSIM.

To validate the effective discharge rate, we need to collect the ground truth discharge rate when affected by a moving bottleneck. To do so, we choose a fixed location (as shown by the star in Figure 7) as the location for observation. A total of six slow-moving trucks are observed on lane 5 and lane 6, between 04:00 p.m. and 04:15 p.m., and between 05:00 p.m. and 05:30 p.m. In other words, we observed a total of six moving bottlenecks. The time-space diagrams of two representative moving bottlenecks, generated by two slower trucks with ID 2862 and 1522, are shown in Figure 9, in which red curves represent trucks, and black curves stand for other general vehicles. For the sake of simplicity, we only show the time-space diagram of two trucks below.

In Figure 9 (a), the slower truck (ID: 2862) is driving in lane 6 at a travel speed of $11\ mph$. Based on the time-space diagram of lane 6, we can tell the slope of the truck trajectory is lower than that of the other vehicles, indicating that the truck is moving slower than the surrounding traffic. It can also be found that the vehicle that follows this truck has a broken trajectory in lane 6, meaning that it chooses to switch to the left lane in order to bypass the slow-moving bottleneck. Based on the time-space diagram, the ground truth discharge rate is found to be approximately $2{,}740\ veh/hr$, for lanes 5 and 6 combined. In

other words, $\mu_{GTD} = 2{,}740\ veh/hr$. Then, the discount factor of the effective discharge rate can be calculated as $\theta = 0.83$, and the effective discharge rate is $\mu' = 2{,}568\ veh/hr$. Comparing μ' and μ_{GTD}, the absolute percentage error (APE) can be calculated as $APE_1 = \frac{|2{,}568-2{,}740|}{2{,}740} = 6.3\%$. On the other hand, if we ignore the impact of the moving bottleneck and directly use the maximum discharge rate μ, by comparing μ and μ_{GTD}, the APE would become $APE_2 = \frac{|3{,}076-2{,}740|}{2{,}740} = 12.3\%$. Comparison of APE_1 and APE_2 suggests that using the proposed effective discharge rate is more reasonable than directly using the maximum discharge rate, and the resulting APE drops from 12.3% to 6.3%.

Figure 9 (b) presents the time space diagram of the moving bottleneck generated by another slower truck (ID: 1522) with a traveling speed of $5\ mphr$. The ground truth discharge rate can be observed and approximately equals $\mu_{GTD} = 1{,}982\ veh/hr$. The effective discharge rate can be calculated as $\mu' = 2{,}127\ veh/hr$. Thus, the APE can be calculated as $APE_1 = \frac{|2{,}127-1{,}982|}{1{,}982} = 9.5\%$, when compared with the ground truth discharge rate. However, the APE will become $APE_2 = \frac{|3{,}076-1{,}982|}{1{,}982} = 55.2\%$ if the impact of the moving bottleneck is ignored. The resulting APE drops from 55.2% to 9.5%, a significant improvement.

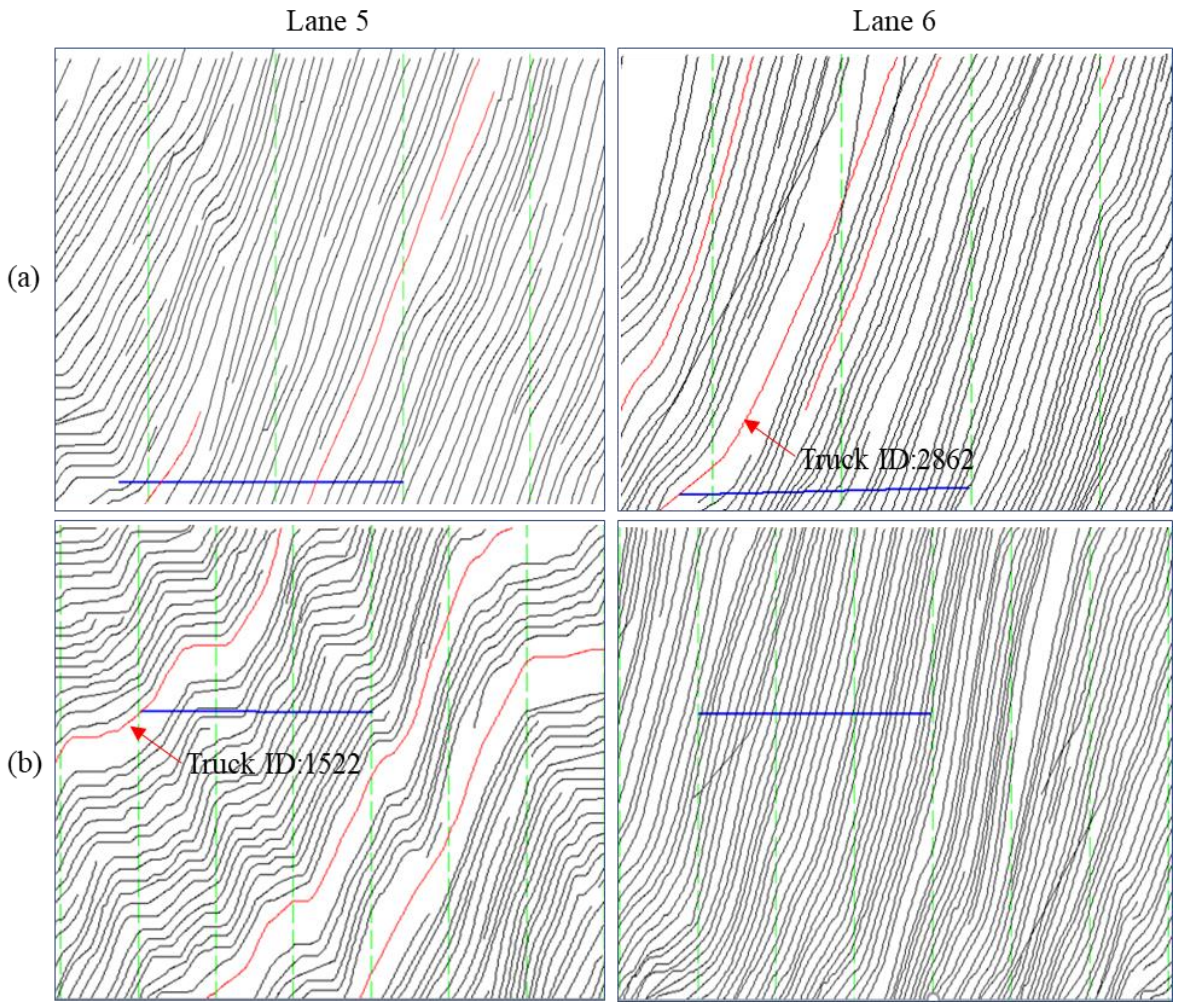

Figure 9. Vehicle trajectory of trucks (IDs:2862 and 1522), I-80, NGSIM.

Figure 10 shows the APE comparison of all six moving bottlenecks caused by those slow-moving trucks. It can be found that the maximum discharge rate μ (represented by the red solid line) always overestimates the ground truth discharge rate μ_{ground} (the black line), with APE_2 (the red dashed line) ranging from 12.3% to 55.2%. On the other hand, the proposed model can calibrate the effective discharge rate μ' (the blue solid line) much closer to the ground truth discharge rate μ_{ground}, with APE_1 (the blue dashed line) ranging from 6.3% to 13.6%. These numbers demonstrate that the proposed model can generate satisfactory traffic capacity associated with moving bottlenecks in traffic flow.

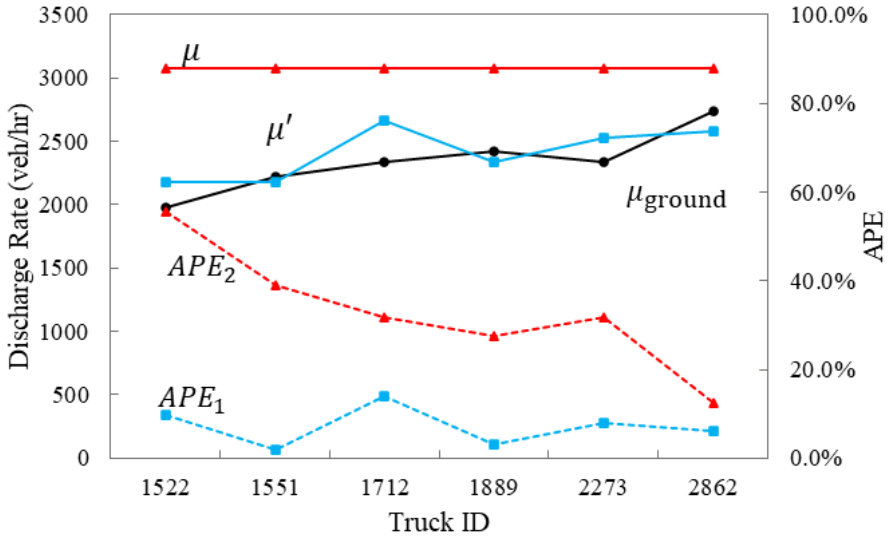

Figure 10. APE comparison of six slower trucks, I-80, NGSIM.

4.2. Typical Scenario ODD Analysis

In this section, we analyze the impact of the ATMA on the traffic flow of a typical highway, including traffic delay and resulting density, to identify the potential ODD of this technology. The analysis target is a four-lane highway segment, as shown in Figure 5. The characteristics of this analyzed highway segment are set as follows: $L = 1\ mile, v_{lt} = 10\ mph, v_u = 50\ mph, w = 12\ mph, k_j = 190\ veh/mile/lane$. Traffic volumes on multilane highways vary widely but often have demand in a range of 15,000 to 40,000 veh/day, while volumes as high as 100,000 veh/day have been observed in some cases [7]. Thus, we set the AADT as ranging from 15,000 veh/day to 60,000 veh/day. Recommended by HCM, the values of representative K, D factors and PHF are set as 0.09, 0.6 and 0.9 to represent urban and rural areas, respectively. The hourly traffic demand can be estimated by Equation 9.

Based on the setup of highway geometry and traffic flow characteristics, the relationship between traffic demand (i.e., AADT), vehicle delay, and traffic density are shown in Figure 11. The average vehicle delay, denoted by the black dotted line, remains zero before the traffic demand AADT reaches 45,000 vehicles per day. After that, the average delay increases sharply from 0 to 36 seconds per vehicle. The red line stands for the traffic density, which increases at a relatively slow speed from 9 veh/mile/lane to 24 veh/mile/lane, when the AADT is no more than 40,000 veh/day. However, after that, the density increases at a much faster pace.

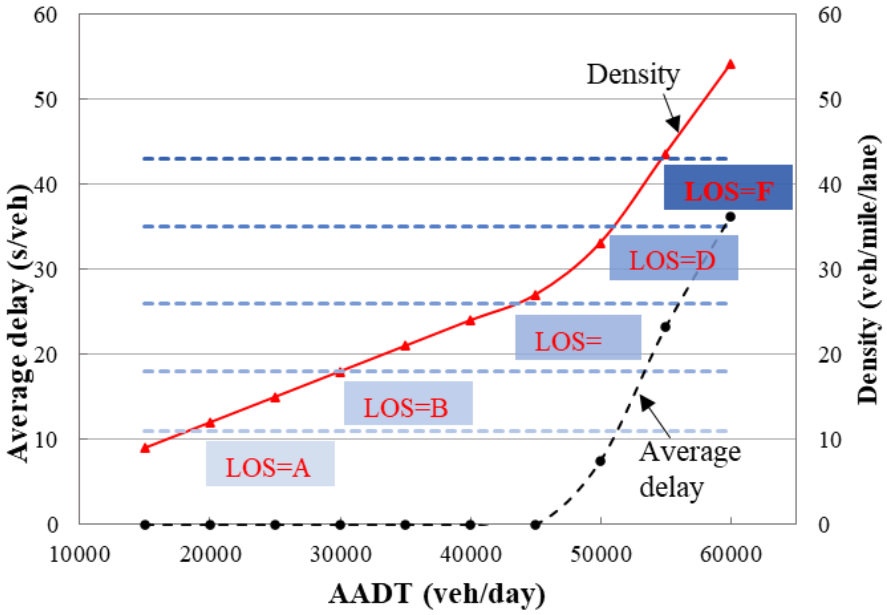

Figure 11. Relationship between AADT, average vehicle delay and traffic density.

We also identify level of service based on density. Learning from Figure 2, the density thresholds that differentiate LOS are 11, 18, 26, 35, and 45, respectively, and we use them to define the LOS category in Figure 11 as well. Figure 2 also tells us that, when LOS is from A to C, the traffic speed does not fluctuate much, and we know that a low speed fluctuation is important for work zone safety. As such, we use LOS=C as a desirable design objective for ATMA's operation design domain, which corresponds to between 40,000 and 45,000 AADT in Figure 11. As can be seen from the figure, when AADT is below 40,000, the delay is zero, where density is relatively low at a value of less than 26 vehicle/lane/mile, and the traffic flow remains at free flow speed. In other words, at this traffic level, drivers do not experience significant traffic disruption and they do not even need to significantly change their speed. As such, for this typical scenario, the AADT of 40,000 is identified as a good threshold for defining ATMA's ODD.

4.3. Sensitivity Analysis

In this section, sensitivity analysis is performed to show how changing the K factor, D factor, and operating speed of ATMA vehicles can influence the total delay and density during maintenance. According to HCM [7], the range of the D factor is set to be 0.5~0.65, with the K factor as 0.08 to 0.11. The operating speeds of ATMA vehicles range from 5~15 mph. Thus, the ODD of the ATMA can be analyzed in accordance with the results of sensitivity analysis.

4.3.1 When D-factor changes

Figure 12 presents the proposed relationship between traffic demand (i.e., AATD), average delay (illustrated in Figure 12-a), and density (illustrated in Figure 12-b), when factor D changes from 0.5 to 0.65.

Figure 12-a shows that, the average delay remains zero at first, but increases sharply once the AADT is beyond a threshold. As we can see, the average delay increases from 0 to 8 sec/veh when D is 0.5, whereas the average delay increases from 0 to 47 sec/veh as D changes to 0.65. The AADT threshold for a delay to start increasing, is about 55,000, when D is 0.5, but as the D value increases, this AADT threshold reduces to 50,000, 45,000, and 40,000, respectively.

Similarly, Figure 12-b shows that the density increases at a much slower speed, until AADT reaches a threshold, after which the density increases much faster. As the D value increases, the traffic flow becomes denser. When D is set to be 0.5, the density increases slightly from 8 veh/mile/lane to 25 veh/mile/lane, and the LOS decreases from A to C before the AADT reaches 50,000 veh/day. Once the AADT is greater than 50,000 veh/day, the density increases significantly from 25 veh/mile/lane to 33 veh/mile/lane, and the LOS becomes worse from C to D. As the D changes to 0.65, the density increases slightly from 10 veh/mile/lane to 26 veh/mile/lane, and the LOS decreases from A to C before the AADT reaches 40,000 veh/day. Once the AADT is greater than 40,000 veh/day, the density increases significantly from 26 veh/mile/lane to 65 veh/mile/lane, and the LOS becomes worse from C to F. Combined from the above analysis, when D factor increases from 0.5, to 0.55, 0.6, and then to 0.65, the corresonding AADT thresholds to define ATMA ODD are 50,000, 45,000, 45,000, and 40,000, respectively.

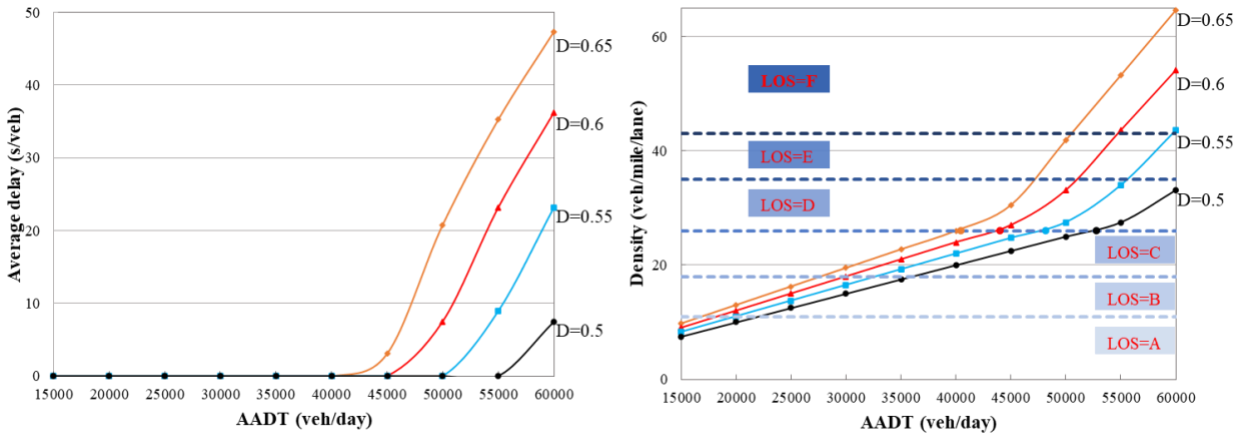

Figure 12. Proposed relationship between AADT and (a) average delay and (b) LOS when D changes.

4.3.2 When K-factor changes

In this section, we examine what will happen if the K factor changes. Figure 13 presents the relationship between traffic demand (i.e., AATD), average delay (illustrated in Figure 13-a) and density (illustrated in Figure 13-b), when K changes from 0.08 to 0.11. The observed pattern is similar with that when D changes.

Figure 13 show that, the average delay and density increases sharply, once the AADT reaches certain thresholds. When K is set to be 0.08, the average delay remains as zero, until the AADT increases to higher than 50,000. After that, the delay increases from 0 to 18 sec/veh. As for the density, it only increases slightly from 8 veh/mile/lane to 24 veh/mile/lane (corresponding to LOS A~C), before the AADT reaches 50,000 veh/day. Once the AADT is higher than that, the density increases significantly from 24 veh/mile/lane to 40 veh/mile/lane, and the LOS becomes worse to E.

Similar trends can also be found for the other curves, corresponding to different K values. In general, when the K value increases, the AADT threshold reduces, and the delay and LOS increases much faster. Combined with these curves, when the K factor increases from 0.08, to 0.09, 0.1 and, then, to 0.11, the corresonding AADT thresholds to define ATMA ODD are 50,000, 45,000, 40,000, and 35,000, respectively.

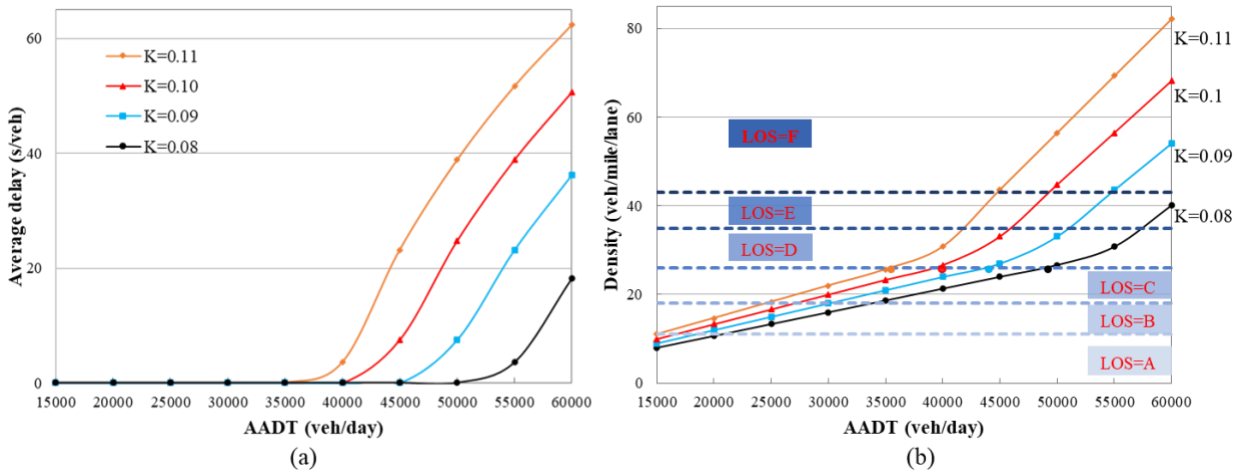

Figure 13. Proposed relationship between the AADT and (a) average delay and (b) LOS when K changes.

4.3.3 When operating speeds of the ATMA vehicles change

In this section, we examine what will happen if an ATMA's operating speed changes. Figure 14 presents the relationship between traffic demand (i.e., AATD), average delay (illustrated in Figure 14-a) and

density (illustrated in Figure 14-b), when the ATMA's operating speed changes from 5 to 15mph. In this analysis, the K is fixed at 0.09 and D is fixed at 0.6. The observed pattern is similar with that when K and D change.

Figure 14-a shows that, the average delay remains zero, if the AADT is less than certain thresholds, which means that the effective discharge rate satisfies the traffic demand. The average delay increases slightly from 7 sec/veh to 17 sec/veh when the ATMA operating speed is set to 15 mph. However, when the operating speed of ATMA vehicles is to be 5 mph, the average delay increases sharply from 0 sec/veh to 109 sec/veh. This is because a slower ATMA operating speed corresponds to a slower moving bottleneck that discounts traffic capacity even more significantly. On the other hand, Figure 14-b shows a similar trend for density, that only increases slightly from 9 veh/mile/lane to 26 veh/mile/lane (corresponding to LOS A~C), before the AADT reaches 45,000 veh/day at an operating speed of 15 mph. If the AADT increases further to exceed this threshold, the resulting density will increase at a much faster pace.

Similar trends can also be found for the other curves that correspond to different ATMA operating speeds. In general, when an operating speed reduces, the AADT threshold reduces, and the delay and LOS increase much faster. Combined with these curves, when operating speeds reduce from 15 mph, to 10 mph and, then, to 5 mph, the corresonding AADT thresholds to define ATMA ODD are 45,000, 45,000, and 40,000, respectively.

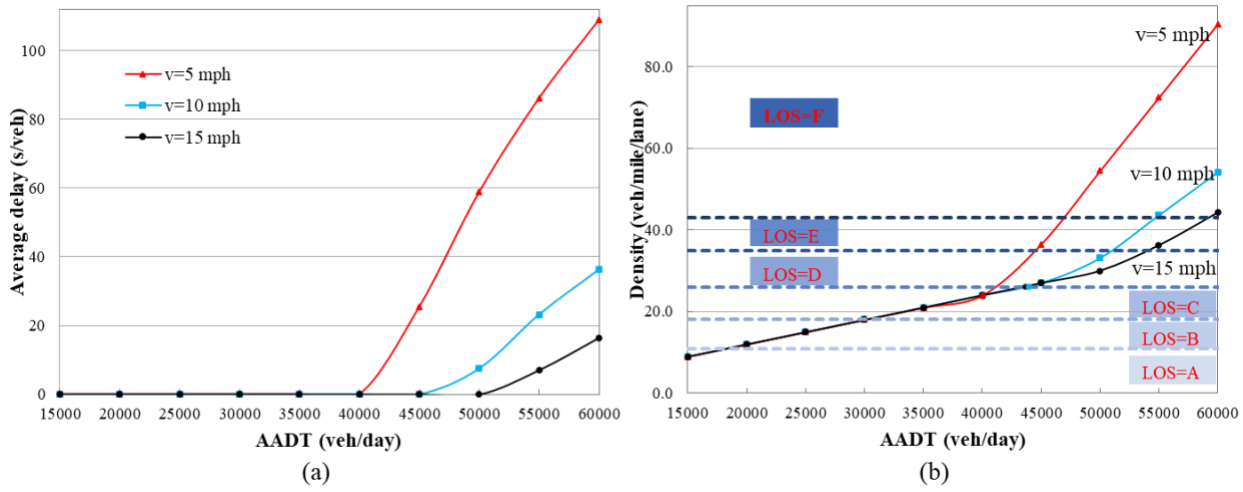

Figure 14. Proposed relationship between the AADT and (a) average delay and (b) LOS when the operating speed of an ATMA changes.

Chapter 5. Conclusion and future research

This study set out to establish the Operational Design Domain for Autonomous Truck Mounted Attenuator systems deployed for roadway maintenance on multilane highways and within work zones. The first step involved the analytical derivation of the effective discharge rate for highway segments impacted by slow-moving ATMA vehicles, which function as moving bottlenecks. This derivation was rooted in a triangular fundamental diagram framework extended to a moving coordinate system. The resulting expressions are simple, closed-form formulas that reflect the influence of traffic demand, instantaneous traffic states, and fundamental flow properties.

Once these discounted capacities were determined, microscopic traffic flow models were applied to estimate associated vehicle delays and density levels. These two metrics, per the Highway Capacity Manual, are fundamental to assessing a highway segment's level of service. This approach enabled the development of a direct analytical link between traffic demand—represented by average annual daily traffic—and LOS. Through this linkage, we were able to numerically explore and define the ODD for ATMA deployments.

Validation using the NGSIM dataset confirmed that the proposed model accurately reflects the reduced discharge rates induced by moving bottlenecks, with estimation errors ranging from 6.3% to 13.6%, which is considered acceptable for operational analysis. For a baseline scenario with parameters K=0.09, D=0.6, and PHF=0.9, the analysis found that LOS=C—a practical design target for ATMA use—corresponds to an AADT threshold of approximately 40,000 vehicles per day. Below this threshold, traffic operations remain close to free-flow conditions, delays are negligible, and vehicle density stays below 26 vehicles per lane per mile. Under such conditions, the presence of an ATMA system is unlikely to impose notable disruptions on driver behavior or travel time, making 40,000 AADT a reasonable benchmark for defining the lower limit of the ODD in typical conditions.

A comprehensive sensitivity analysis was also conducted to assess how variations in the K factor, D factor, and ATMA travel speed affect system performance. Results confirmed that changes in these parameters shift the AADT threshold accordingly, demonstrating that the ODD is context-dependent and should be adjusted to reflect varying traffic environments.

References

1. ASCE. Report Card for America's Infrastructure 2020; Available from: https://infrastructurereportcard.org/cat-item/roads/.

2. MoDOT, Leader-Follower Truck Mounted Attenuator System Request for Proposal. 2018, Missouri Department of Transportation: Jefferson City, Missouri.

3. Skip Descant, Colorado DOT Launches Autonomous Vehicles to Improve Worker Safety. 2017; Available from: https://www.govtech.com/fs/data/Colorado-DOT-Launches.

4. Tang, Q., Y. Cheng, X. Hu, C. Chen, Y. Song, and R. Qin, Evaluation Methodology of Leader-Follower Autonomous Vehicle System for Work Zone Maintenance. Transportation Research Record, 2021. 0(0): p. 0361198120985233.

5. Inc., R.T.E. Autonomous TMA Truck to Provide Insights to TDOT for Improving Work Zone Safety. 2019; Available from: https://www.prnewswire.com/news-releases/autonomous-tma-truck-to-provide-insights-to-tdot-for-improving-work-zone-safety-300951862.html.

6. CDOT. Autonomous Maintenance Technology (AMT) Pool Fund. 2018; Available from: http://www.csits.colostate.edu/autonomous-maintenance-technology.html.

7. Highway Capacity Manual. 2010: Transportation Reseach Board.

8. Leclercq, L., J.A. Laval, and N. Chiabaut, Capacity Drops at Merges: an endogenous model. Procedia - Social and Behavioral Sciences, 2011. 17: p. 12-26.

9. Leclercq, L., V.L. Knoop, F. Marczak, and S.P. Hoogendoorn, Capacity drops at merges: New analytical investigations. Transportation Research Part C: Emerging Technologies, 2016. 62: p. 171-181.

10. Leclercq, L., F. Marczak, V.L. Knoop, and S.P. Hoogendoorn, Capacity Drops at Merges: Analytical Expressions for Multilane Freeways. Transportation Research Record, 2016. 2560(1): p. 1-9.

11. Yuan, K., V.L. Knoop, and S.P. Hoogendoorn, A Microscopic Investigation Into the Capacity Drop: Impacts of Longitudinal Behavior on the Queue Discharge Rate. Transportation Science, 2017. 51(3): p. 852-862.

12. Laval, J.A. and C.F. Daganzo, Lane-changing in traffic streams. Transportation Research Part B: Methodological, 2006. 40(3): p. 251-264.

13. Chen, D. and S. Ahn, Capacity-drop at extended bottlenecks: Merge, diverge, and weave. Transportation Research Part B: Methodological, 2018. 108: p. 1-20.

14. Menendez, M. and C.F. Daganzo, Effects of HOV lanes on freeway bottlenecks. Transportation Research Part B: Methodological, 2007. 41(8): p. 809-822.

15. Laval, J.A. and L. Leclercq, Microscopic modeling of the relaxation phenomenon using a macroscopic lane-changing model. Transportation Research Part B: Methodological, 2008. 42(6): p. 511-522.

16. Monamy, T., H. Haj-Salem, and J.-P. Lebacque, A Macroscopic Node Model Related to Capacity Drop. Procedia - Social and Behavioral Sciences, 2012. 54: p. 1388-1396.

17. Parzani, C. and C. Buisson, Second-Order Model and Capacity Drop at Merge. Transportation Research Record, 2012. 2315(1): p. 25-34.

18. Jin, W.-L., Q.-J. Gan, and J.-P. Lebacque, A kinematic wave theory of capacity drop. Transportation Research Part B: Methodological, 2015. 81: p. 316-329.

19. Newell, G.F., A simplified car-following theory: a lower order model. Transportation Research Part B: Methodological, 2002. 36(3): p. 195-205.

20. Newell, G.F., Applications of Queueing Theory. Ettore Majorana International Science Series. 1982: Springer Netherlands.

21. Newell, G.F., A moving bottleneck. Transportation Research Part B: Methodological, 1998. 32(8): p. 531-537.

22. Zhou, X. and J. Taylor, DTALite: A queue-based mesoscopic traffic simulator for fast model evaluation and calibration. Cogent Engineering, 2014. 1(1): p. 961345.